

# Structural data from X-ray powder diffraction for new high-temperature phases $(Y_{1-x}Ln_x)_2Si_2O_7$ with $Ln = Ce, Pr, Nd$

F. Monteverde\*, G. Celotti

*Research Institute for Ceramics Technology, Via Granarolo, 64, 48018 Faenza (RA), Italy*

Received 17 January 2001; received in revised form 14 May 2001; accepted 20 May 2001

## Abstract

Extending the investigation on possible mixed phases with composition  $(Y_{1-x}Ln_x)_2Si_2O_7$  formed at high temperature under oxidizing conditions in silicon nitride samples doped with  $Y_2O_3$  and  $Ln_2O_3$  as sintering aids, the compounds with  $Ln = Ce, Pr, Nd$  were successfully synthesized and structurally characterized by Rietveld whole powder pattern refinement. Some fluctuations in the  $x$  values were found as well, but all the compounds are monoclinic (space group  $P2_1/c$ ), with lattice parameters close to those of the previously studied  $(Y_{2/3}La_{1/3})_2Si_2O_7$ . Further efforts with Sm (and Dy) failed in producing the expected G-form phase, indicating that the family does not extend beyond Nd: in these cases Ln ions partially substitute Y in its already known  $\alpha$ - and  $\delta$ -disilicates. Under the adopted experimental conditions (1 atm, ambient air), an explanation of the impossibility to obtain the phase in question containing lanthanides with  $Z \geq 62$  was attempted on the basis of lattice strains introduced by foreign ions larger than Y. © 2002 Elsevier Science Ltd. All rights reserved.

**Keywords:**  $(Y, Ln)_2Si_2O_7$ ; X-ray methods; Phase composition; Grain boundary phase

## 1. Introduction

During previous studies of the oxidation resistance at high temperature in air of fully dense silicon nitride based materials densified with the addition of sintering aids (i.e.  $Y_2O_3$  and  $La_2O_3$ ), a new mixed disilicate was found and completely characterized.<sup>1</sup> A synthesis of this new phase, out of a silicon nitride matrix, was successfully carried out as well in excess of  $SiO_2$ .

To improve the knowledge of such  $(Y_{1-x}Ln_x)_2Si_2O_7$  possible class of compounds with high temperature G-form structure,<sup>2,3</sup> a systematic study with following light rare earths ( $Ln = Ce, Pr, Nd, Sm$ ) was undertaken. Experiments were performed with  $Ln = Dy$  too, even if this element does not belong properly to the light group, due to the fact that its ionic radius is almost equal to that of  $Y^{3+}$ .

This paper describes the synthesis of these new mixed disilicates, the assessment of their stoichiometry and the relative structure determination. When the expected phase failed to form, the reasons for this finding were analyzed and tentatively explained.

## 2. Experimental

Several powder mixtures were prepared varying the molar content of the rare earth oxides involved ( $Y_2O_3$ , H.C. Starck - Germany;  $CeO_2$ , Merck - Germany;  $Pr_6O_{11}$ ,  $Nd_2O_3$ ,  $Sm_2O_3$ ,  $Dy_2O_3$ , Techsnabexport - Russia), the test temperature and the dwell time in view to obtain the highest amount and/or the best defined X-ray diffraction pattern of the expected new mixed disilicate. The prerequisite of the amorphous silica ( $SiO_2$ , Carlo Erba - Italy) in excess was kept constant for each prepared mixture.

Once the initial composition was designed, the oxide precursors were ultrasonically mixed in pure ethanol and dried. The blend was then softly pestled in agate mortar, pelletized ( $100 \text{ kg/cm}^2$ ), mounted on a platinum support, and finally placed in a laboratory kiln.

The as-treated pellet was finely ground in agate mortar and, on this powdered sample, the XRD analyses were conducted. Accurate XRD patterns were recorded over an angular range  $10^\circ < 2\theta < 60^\circ$  on a Siemens mod. D500 (Ni filtered  $CuK_\alpha$ , 25 mA 33 KV, step width  $0.02^\circ$ , sampling time 6 s). Table 1 summarizes the most significant attempts with starting composition, thermal cycle and crystalline phases identified.

\* Corresponding author.

E-mail address: federico@irtec1.irtec.bo.cnr.it (F. Monteverde).

Parallel inspections were performed via SEM (Cambridge mod. S360) equipped with an EDX analyzer (eXL II Link Analytical Pentafet) in order to assess the composition associated to the new formed phases. For this need it was necessary to coat the selected powdered samples with a thin carbon film.

The experimental diffraction patterns were processed using the following software packages: DBWS-9411 for Rietveld refinement,<sup>4</sup> DMPLOT<sup>5</sup> and PowderCell 2.3<sup>6</sup> for the necessary graphic illustrations.

### 3. Results and discussion

Being the expected structure type of the possible  $(Y_{1-x}Ln_x)_2Si_2O_7$  phases known from the early determined  $(Y_{2/3}La_{1/3})_2Si_2O_7$ ,<sup>1</sup> a systematic search was carried out on

mixtures thermally treated at different temperatures from 1400 to 1650°C.

By varying the starting compositions, as shown in Table 1, the G-form structure was clearly identified in some Ce-, Pr- and Nd-containing samples. In the first three Nd-containing samples, this form is not detectable due to the fact that, even if small quantities would have been present, the overlapping peaks of  $\alpha$ - or  $\delta$ - $Y_2Si_2O_7$  made the identification largely uncertain. Quantitative EDX analyses yielded for Ce a stoichiometry very similar to the La compound,<sup>1</sup> i.e.  $X \approx 1/3$ , while for Pr  $X \approx 1/2$  was found and for Nd  $X \approx 2/5$ , with no traces of other phases, excluding the unavoidable  $SiO_2$  ( $\alpha$ -cristobalite).

On the contrary the Sm-containing samples resisted to any effort: at temperatures 1400–1500°C only  $\alpha$ - $Y_2Si_2O_7$ , and  $\delta$ - $Y_2Si_2O_7$  at temperatures 1550–1650°C were detected. A careful inspection of the XRD patterns revealed

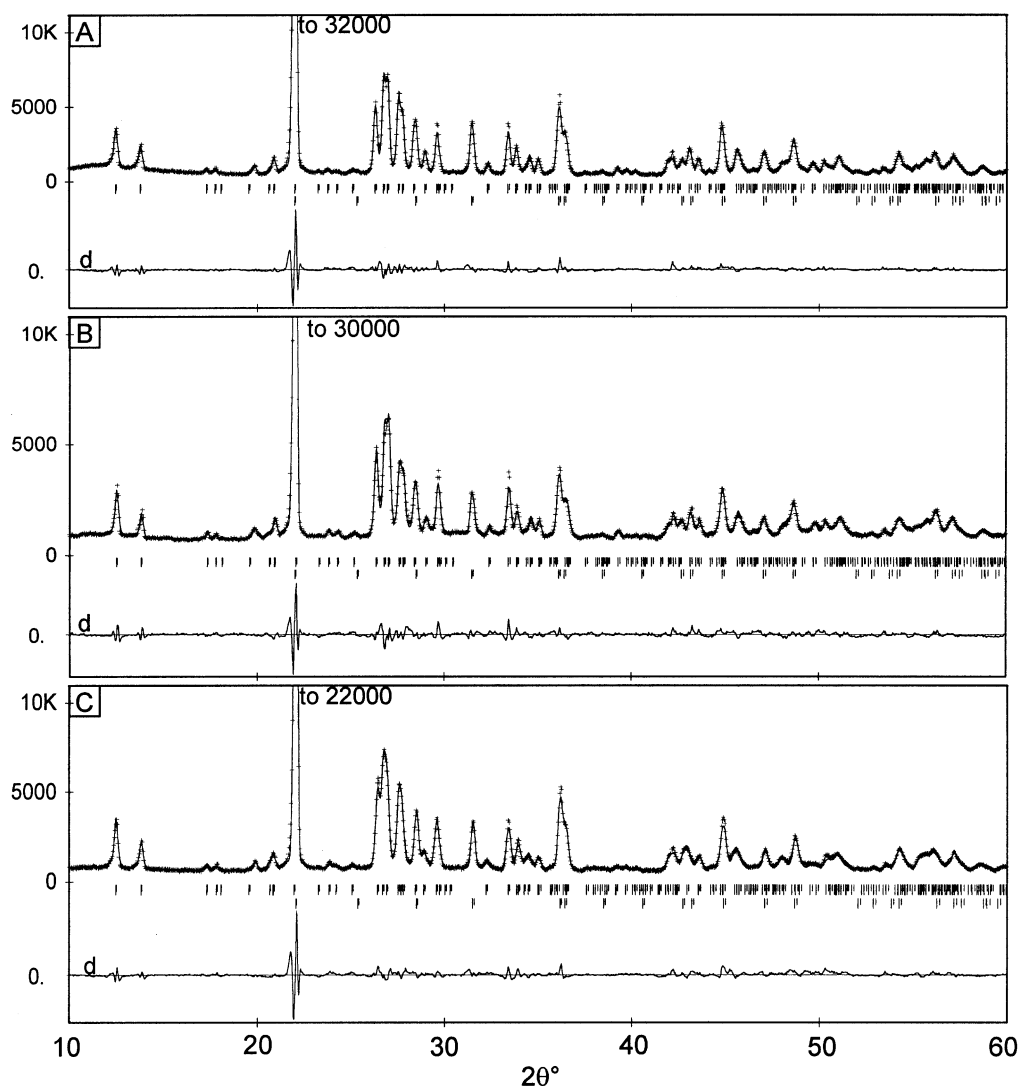


Fig. 1. Outputs of the whole-powder-X ray pattern fitting by Rietveld refinement [observed profile intensities (+) and calculated intensities (-)] for the selected compositions YCe3 (A), YPr5 (B), and YNd4 (C). The difference plot (d) between the observed and calculated intensities for each processed XRD patterns is shown. Short vertical bars represent the Bragg reflection positions of the expected new phase (upper) and  $\alpha$ -cristobalite (lower)

that lattice parameters of the two Y-disilicates increased on the average by about 1% ( $\alpha$ -form:  $a=6.62$ ,  $b=6.71$ ,  $c=12.34$  Å,  $\alpha=94$ ,  $\beta=89$ ,  $\gamma=93^\circ$ ;  $\delta$ -form:  $a=13.81$ ,  $b=5.02$ ,  $c=8.30$  Å), indicating that Sm substituted partially for Y: instead of forming the expected phase, Sm prefers to occupy Y sites in both the well known disilicate polymorphs.<sup>7</sup>

While La, Ce, Pr and Nd elements have ionic radius  $r$  exceeding that of Y by more than 10% (corresponding to a volume increase  $\geq 33\%$  in large cations fraction,

representing 8–12% of the total cell volume), Sm is the first with  $r$  going below this limit: it seems that, when the linear strain induced by the substitution of Y by Ln element is lower than 10%, the lanthanide enters the Y-disilicate lattice (corresponding to the thermal treatment temperature) and does not give rise to G-form structure anymore.

A further experiment was performed with Dy, which exhibits a linear lattice strain, if compared to Y, of merely  $\sim 1\%$ : such a element is the last showing a  $\delta$ -type disilicate among the lanthanides: mainly  $\delta$ -(Y,Dy) $_2$ Si $_2$ O $_7$  and traces of  $\gamma$ -(Y,Dy) $_2$ Si $_2$ O $_7$  were found with lattice parameters increased on the average by 0.1% ( $a=13.70$ ,  $b=5.01$ ,  $c=8.18$  Å). Strong evidence can be deduced for the fact that (Y $_{1-x}$ Ln $_x$ ) $_2$ Si $_2$ O $_7$  compounds with high temperature G-type structure are formed only with rare earth types characterized by a ionic radius sufficiently large.

The structural data for the isomorphous new compounds (Y $_{2/3}$ Ce $_{1/3}$ ) $_2$ Si $_2$ O $_7$ , (Y $_{1/2}$ Pr $_{1/2}$ ) $_2$ Si $_2$ O $_7$  and (Y $_{3/5}$ Nd $_{2/5}$ ) $_2$ Si $_2$ O $_7$  are reported in Tables 2–5. The results of the whole-powder-pattern fitting are presented in Fig. 1a–c for the new formed high temperature Ln–Y disilicates, Ln = Ce(a), Pr(b), Nd(c). The comparison between observed and calculated intensities are shown in Tables 6–8 (excluded the reflections belonging to  $\alpha$ -cristobalite). These outputs were obtained after Rietveld refinement by means of the DBWS-9411 program,<sup>4</sup> starting from structural parameters predetermined for (Y $_{2/3}$ La $_{1/3}$ ) $_2$ Si $_2$ O $_7$  (Table 5). The drawings in Fig. 2a–c, built with PowderCell 2.3<sup>6</sup> represent the projection of the monoclinic (Y $_{1-x}$ Ln $_x$ ) $_2$ Si $_2$ O $_7$  structure with Ln = Ce (a), Pr (b), and Nd (c).

The reliability index  $R_{WP}$  is quite good (Table 5), even if not as satisfactory as in the case of La: from Tables 2–4 it can be noted again the tendency of Y to occupy preferentially positions (2) leaving the major part of substituting Ln in position (1). In the case of Pr, the sharing is complete, with Y and Pr occupying in equal proportions position (2) and (1), respectively.

SEM micrographs from some as-treated powder mixtures and corresponding EDX spectra are presented in Fig. 3.

The apparent deviation of Pr-based compound cell volume from the expected monotonic decrease, coming from the well known “lanthanide contraction”, is easily understood taking into account the fact that larger Pr ions substitute Y in an anomalously high proportion.

The reason why more Ln enters in the compound (Y $_{1-x}$ Ln $_x$ ) $_2$ Si $_2$ O $_7$  when Ln = Pr, Nd is not easy to understand. It seems that a sort of volume compensating mechanism is activated which prevents the cell volume from becoming too small (allow for the fact that all the cell volumes of the new mixed phases lie within a poor 1.5%).

Theoretical calculations based on the volumes of the different ions involved in the formula units treated as cubes of edge  $2r$  yielding a complete space filling, properly

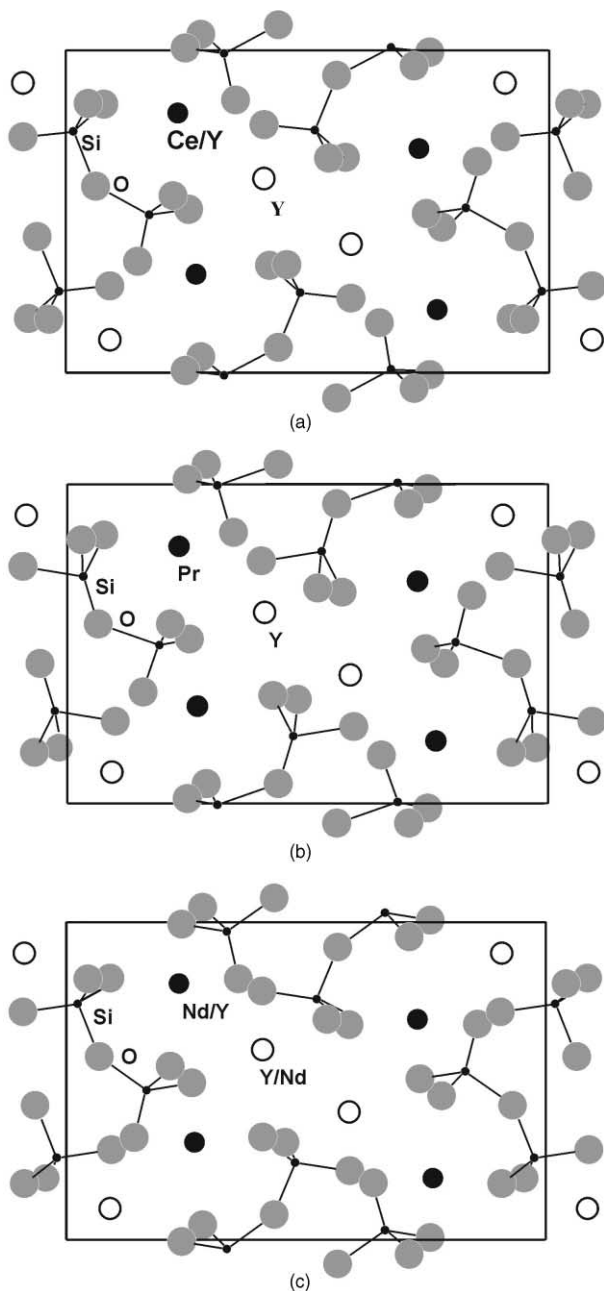


Fig. 2. Projection of the monoclinic structure (space group  $P2_1/c$ ) seen along  $[100]$  at  $(10\bar{1})$  of (Y $_{2/3}$ Ce $_{1/3}$ ) $_2$ Si $_2$ O $_7$  (a), (Y $_{1/2}$ Pr $_{1/2}$ ) $_2$ Si $_2$ O $_7$  (b), and (Y $_{3/5}$ Nd $_{2/5}$ ) $_2$ Si $_2$ O $_7$  (c).

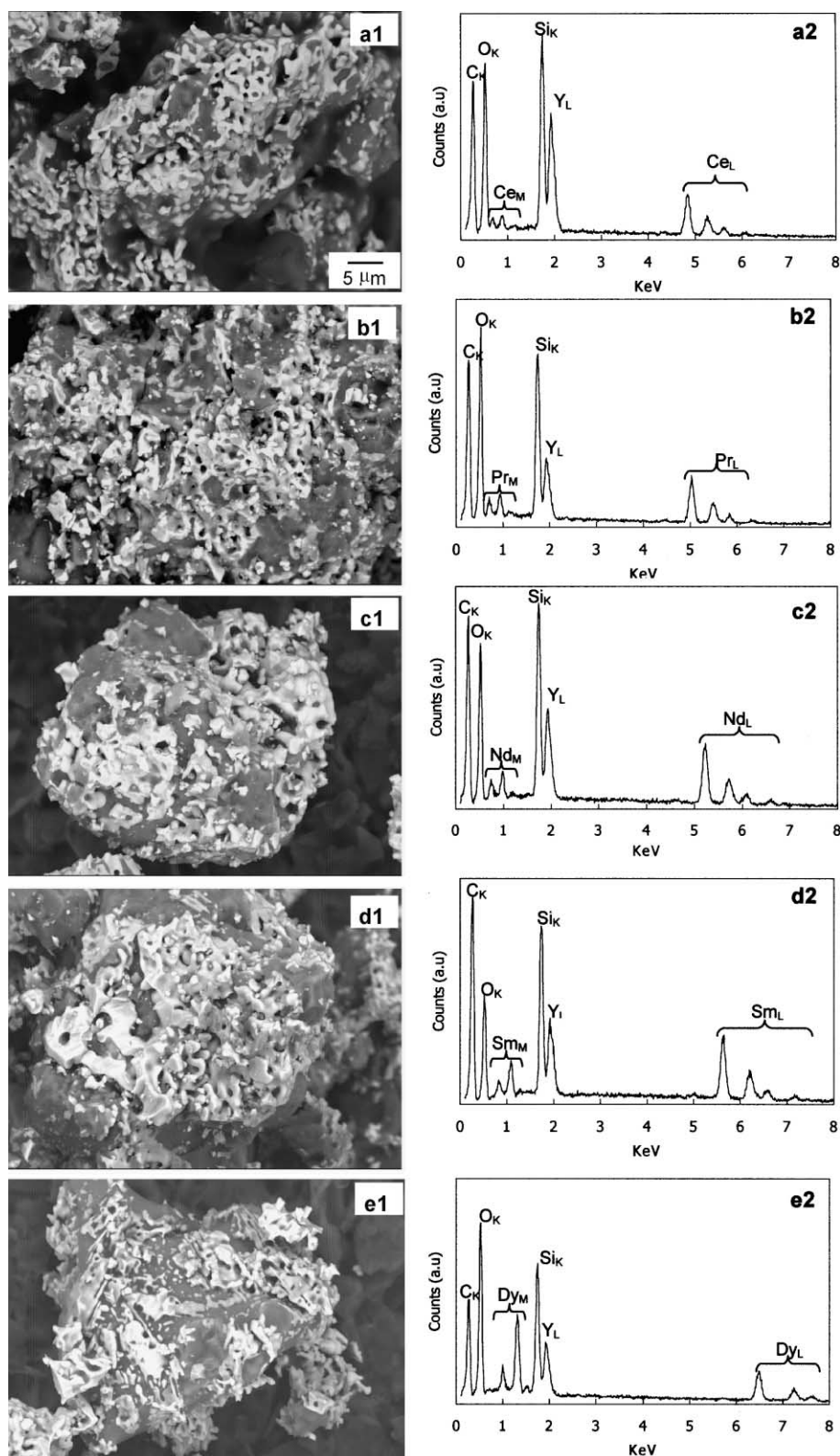


Fig. 3. BSE-SEM micrographs (left column) from the as treated mixtures YCe2 (a1), YPr6 (b1), YNd5 (c1), YSm4 (d1), and YDy1 (e1). The EDX spectra (right column) were collected on the bright features (placed upon the grey  $\alpha$ -cristobalite particles) of the corresponding micrograph.

Table 1

Summary of the most significant attempts: the complement to 100% (wt. or mol) for each composition consists of amorphous silica

| Mixture | Composition |      |      |      | Thermal treatment   |              | Crystalline phases |                        |                                                                                                                                                 | Notes |
|---------|-------------|------|------|------|---------------------|--------------|--------------------|------------------------|-------------------------------------------------------------------------------------------------------------------------------------------------|-------|
|         | Y           |      | Ln   |      | Temperature<br>(°C) | dwell<br>(h) | NSP <sup>c</sup>   | $\alpha$ -cristobalite |                                                                                                                                                 |       |
|         | wt.%        | mol% | wt.% | mol% |                     |              |                    |                        |                                                                                                                                                 |       |
| YPr1    | 6           | 2    | 24   | 2    | 1450                | 2            | Y <sup>d</sup>     | Y                      | Y <sub>2</sub> SiO <sub>5</sub> * <sup>a</sup>                                                                                                  |       |
| YPr2    | 15          | 5.3  | 15   | 1.2  | 1500                | 2            | Y                  | Y                      | $\delta$ -Y <sub>2</sub> Si <sub>2</sub> O <sub>7</sub>                                                                                         |       |
| YPr3    | 6           | 2    | 24   | 2    | 1500                | 2            | Y                  | Y                      | —                                                                                                                                               |       |
| YPr4    | 10          | 1.6  | 20   | 3.6  | 1500                | 2            | Y                  | Y                      | —                                                                                                                                               |       |
| YPr5    | 6           | 2    | 24   | 2    | 1550                | 2            | Y                  | Y                      | —                                                                                                                                               | **b   |
| YPr6    | 10          | 1.6  | 20   | 3.6  | 1550                | 2            | Y                  | Y                      | —                                                                                                                                               |       |
| YPr7    | 15          | 5.3  | 15   | 1.2  | 1600                | 2            | —                  | Y                      | $\delta$ -Y <sub>2</sub> Si <sub>2</sub> O <sub>7</sub>                                                                                         | Fused |
| YCe1    | 14.1        | 5    | 20.3 | 9.2  | 1450                | 2            | Y                  | Y                      | Y <sub>2</sub> SiO <sub>5</sub> *, CeO <sub>2</sub>                                                                                             |       |
| YCe2    | 15          | 6.6  | 15   | 5.0  | 1500                | 2            | Y                  | Y                      | —                                                                                                                                               |       |
| YCe3    | 15          | 6.6  | 15   | 5.0  | 1550                | 2            | Y                  | Y                      | —                                                                                                                                               | **    |
| YCe4    | 14.1        | 5    | 20.3 | 9.2  | 1550                | 2            | Y                  | Y                      | —                                                                                                                                               |       |
| YCe5    | 15          | 6.6  | 15   | 5.0  | 1600                | 2            | —                  | Y                      | $\delta$ -Y <sub>2</sub> Si <sub>2</sub> O <sub>7</sub>                                                                                         | Fused |
| YNd1    | 15          | 5.2  | 15   | 3.5  | 1450                | 2            | —                  | Y                      | $\alpha$ -Y <sub>2</sub> Si <sub>2</sub> O <sub>7</sub>                                                                                         |       |
| YNd2    | 15          | 5.2  | 15   | 3.5  | 1500                | 2            | —                  | Y                      | $\alpha$ -Y <sub>2</sub> Si <sub>2</sub> O <sub>7</sub>                                                                                         |       |
| YNd3    | 15          | 5.2  | 15   | 3.5  | 1550                | 2            | —                  | Y                      | $\delta$ -Y <sub>2</sub> Si <sub>2</sub> O <sub>7</sub>                                                                                         |       |
| YNd4    | 14          | 5.1  | 21   | 5.2  | 1550                | 2            | Y                  | Y                      | —                                                                                                                                               | **    |
| YNd5    | 18          | 4.2  | 12   | 4.2  | 1600                | 2            | Y                  | Y                      | $\delta$ -Y <sub>2</sub> Si <sub>2</sub> O <sub>7</sub>                                                                                         |       |
| YNd6    | 14          | 5.1  | 21   | 5.2  | 1600                | 2            | Y                  | Y                      | —                                                                                                                                               |       |
| YSm1    | 10          | 3.5  | 20   | 4.5  | 1400                | 2            | —                  | Y                      | $\alpha$ -Y <sub>2</sub> Si <sub>2</sub> O <sub>7</sub>                                                                                         |       |
| YSm2    | 15          | 5.2  | 15   | 3.4  | 1450                | 2            | —                  | Y                      | $\alpha$ -Y <sub>2</sub> Si <sub>2</sub> O <sub>7</sub>                                                                                         |       |
| YSm3    | 15          | 5.2  | 15   | 3.4  | 1500                | 2            | —                  | Y                      | $\alpha$ -(Y,Sm) <sub>2</sub> Si <sub>2</sub> O <sub>7</sub>                                                                                    |       |
| YSm4    | 15          | 5.2  | 15   | 3.4  | 1550                | 2            | —                  | Y                      | $\delta$ -(Y,Sm) <sub>2</sub> Si <sub>2</sub> O <sub>7</sub> , Sm <sub>2</sub> O <sub>3</sub> /Sm <sub>2</sub> Si <sub>2</sub> O <sub>7</sub> * |       |
| YSm5    | 14          | 5.1  | 21   | 5.2  | 1550                | 2            | —                  | Y                      | $\delta$ -(Y,Sm) <sub>2</sub> Si <sub>2</sub> O <sub>7</sub> , Sm <sub>2</sub> O <sub>3</sub> /Sm <sub>2</sub> Si <sub>2</sub> O <sub>7</sub> * |       |
| YSm6    | 10          | 3.5  | 20   | 4.5  | 1600                | 2            | —                  | Y                      | $\delta$ -(Y,Sm) <sub>2</sub> Si <sub>2</sub> O <sub>7</sub> , Sm <sub>2</sub> O <sub>3</sub> /Sm <sub>2</sub> Si <sub>2</sub> O <sub>7</sub> * |       |
| YSm7    | 10          | 3.5  | 20   | 4.5  | 1650                | 2            | —                  | Y                      | $\delta$ -(Y,Sm) <sub>2</sub> Si <sub>2</sub> O <sub>7</sub> , Sm <sub>2</sub> O <sub>3</sub> /Sm <sub>2</sub> Si <sub>2</sub> O <sub>7</sub> * |       |
| YDy1    | 18.7        | 5    | 11.3 | 5    | 1600                | 2            | —                  | Y                      | $\delta$ -(Y,Dy) <sub>2</sub> Si <sub>2</sub> O <sub>7</sub> , $\gamma$ -(Y,Dy) <sub>2</sub> Si <sub>2</sub> O <sub>7</sub> *                   |       |

<sup>a</sup> \* Traces.<sup>b</sup> \*\* Pattern processed for Rietveld refinement.<sup>c</sup> NSP: new synthesized phase.<sup>d</sup> Y: yes.

Table 2

Structural data of the new phase (Y<sub>2/3</sub>Ce<sub>1/3</sub>)<sub>2</sub>Si<sub>2</sub>O<sub>7</sub><sup>a</sup>

| Atom  | X      | Y      | Z      | Occupancy |
|-------|--------|--------|--------|-----------|
| Y(1)  | 0.5172 | 0.8055 | 0.7689 | 0.335     |
| Ce(1) |        |        |        | 0.665     |
| Y(2)  | 0.8295 | 0.6008 | 0.5890 | 1         |
| Si(1) | 0.730  | 0.253  | 0.014  | 1         |
| Si(2) | 0.910  | 0.510  | 0.171  | 1         |
| O(1)  | 0.806  | 0.421  | 0.059  | 1         |
| O(2)  | 0.999  | 0.164  | 0.045  | 1         |
| O(3)  | 0.574  | 0.168  | 0.078  | 1         |
| O(4)  | 0.560  | 0.268  | 0.910  | 1         |
| O(5)  | 0.798  | 0.493  | 0.253  | 1         |
| O(6)  | 0.231  | 0.451  | 0.221  | 1         |
| O(7)  | 0.034  | 0.655  | 0.150  | 1         |

<sup>a</sup> B<sub>OV</sub> = 0.4.

Table 3

Structural data of the new phase (Y<sub>1/2</sub>Pr<sub>1/2</sub>)<sub>2</sub>Si<sub>2</sub>O<sub>7</sub><sup>a</sup>

| Atom  | X      | Y      | Z      | Occupancy |
|-------|--------|--------|--------|-----------|
| Pr(1) | 0.5161 | 0.8044 | 0.7688 | 1         |
| Y(2)  | 0.8371 | 0.5988 | 0.5876 | 1         |
| Si(1) | 0.753  | 0.289  | 0.028  | 1         |
| Si(2) | 0.928  | 0.505  | 0.186  | 1         |
| O(1)  | 0.801  | 0.438  | 0.059  | 1         |
| O(2)  | 0.009  | 0.174  | 0.025  | 1         |
| O(3)  | 0.597  | 0.161  | 0.072  | 1         |
| O(4)  | 0.540  | 0.258  | 0.903  | 1         |
| O(5)  | 0.790  | 0.484  | 0.249  | 1         |
| O(6)  | 0.288  | 0.439  | 0.215  | 1         |
| O(7)  | 0.019  | 0.650  | 0.159  | 1         |

<sup>a</sup> B<sub>OV</sub> = 1.5.

Table 4  
Structural data of the new phase  $(Y_{3/5}Nd_{2/5})_2Si_2O_7^a$

| Atom  | X      | Y      | Z      | Occupancy |
|-------|--------|--------|--------|-----------|
| Y(1)  | 0.5234 | 0.8056 | 0.7662 | 0.5       |
| Nd(1) |        |        |        | 0.5       |
| Y(2)  | 0.8346 | 0.5984 | 0.5889 | 0.7       |
| Nd(2) |        |        |        | 0.3       |
| Si(1) | 0.745  | 0.258  | 0.021  | 1         |
| Si(2) | 0.920  | 0.530  | 0.164  | 1         |
| O(1)  | 0.811  | 0.422  | 0.066  | 1         |
| O(2)  | 0.018  | 0.194  | 0.046  | 1         |
| O(3)  | 0.577  | 0.176  | 0.090  | 1         |
| O(4)  | 0.542  | 0.282  | 0.908  | 1         |
| O(5)  | 0.854  | 0.507  | 0.260  | 1         |
| O(6)  | 0.297  | 0.453  | 0.216  | 1         |
| O(7)  | 0.043  | 0.678  | 0.142  | 1         |

<sup>a</sup>  $B_{OV} = 0.7$ .

account for unit cell volumes found in the given stoichiometry: the monotonic reduction in  $O^{2-}$  radius with decreasing trivalent cations size observed in lanthanides pyrosilicates has to be held in due consideration, being oxygen responsible of about 90% of cell volume occupation.

The overall thermal factor  $B_{OV}$  significantly higher for Pr compound (Table 3) has likely to be attributed to the lower stability of Pr oxides.

The best fit implies not negligible displacements of some oxygen atoms from the geometrically regular tetrahedral positions, leading to a typical distorted arrangement linked to the non-equilibrium conditions of nucleation and growth. On the other hand the spatial positions of the heavy ions in the real lattice remain remarkably constant, and those of Si undergo only minor changes (Tables 2–4). In general, the partial substitution of Y to Ln ions, doesn't introduce substantial modification in the G-form structure as described in Refs [2] and [3] (accounting for the choice in Ref. [3] of a description by  $P2_1/n$  space group with  $\beta$  very close to  $90^\circ$ ), apart from the enhanced tetrahedra distortion. An estimate of  $SiO_4$  tetrahedra distortion, based both on the discrepancy of Si–O average bond distances as compared to the theoretical value (1.65 Å) and on the half maximum spread of the same

distance, gave 11% for La, 8% for Ce, 15% for Pr and 6% for Nd compounds, respectively. Once more Pr, besides the peculiar Ln-rich stoichiometry, involves the most perturbed structure.

While Y-La compound is white, Y-Ce appears very pale yellow, Y-Pr very pale green and Y-Nd very pale purple coloured: of course the colours are faded by the contemporary presence of large fraction of white  $SiO_2$  ( $\alpha$ -cristobalite).

#### 4. Conclusions

Extending the study of the class of compounds  $(Y_{1-x}Ln_x)_2Si_2O_7$  with high temperature G-form structure, whose first member was that with Ln = La and  $X = 1/3$ , three new phases were synthesized (with Ln = Ce, Pr, Nd and  $X = 1/3, 1/2, 2/5$  respectively) in excess of silica, and structurally characterized by whole powder X-ray pattern Rietveld refinement. All the new phases are monoclinic, space group  $P2_1/c^{(14)}$ , with cell parameters as follows ( $Z = 4$  for everyone):  $(Y_{2/3}Ce_{1/3})_2Si_2O_7$ ,  $a = 5.365(1)\text{Å}$ ,  $b = 8.509(1)\text{Å}$ ,  $c = 13.804(1)\text{Å}$ ,  $\beta = 111.45(1)^\circ$ ,  $\rho_{XRD} = 4.305\text{ g/cm}^3$ ;  $(Y_{1/2}Pr_{1/2})_2Si_2O_7$ ,  $a = 5.370(1)\text{Å}$ ,  $b = 8.542(2)\text{Å}$ ,  $c = 13.838(2)\text{Å}$ ,  $\beta = 111.76(2)^\circ$ ,  $\rho_{XRD} = 4.485\text{ g/cm}^3$ ;  $(Y_{3/5}Nd_{2/5})_2Si_2O_7$ ,  $a = 5.362(1)\text{Å}$ ,  $b = 8.496(1)\text{Å}$ ,  $c = 13.782(1)\text{Å}$ ,  $\beta = 111.46(1)^\circ$ ,  $\rho_{XRD} = 4.435\text{ g/cm}^3$ .

In these cases too the atomic coordinates showed that substitution of Ln for Y cations preferentially occurs in half of the possible lattice positions: only Nd presents replacement in both of them. Si-O tetrahedra are slightly distorted in Ce and Nd compounds, while Pr compound is characterized by a deformation even larger than that previously found for La.

Attempts to obtain the high temperature G-form phase with Ln = Sm, Dy failed, probably because the lanthanides more easily substituted Y in  $\alpha$ - and/or  $\delta$ -disilicates lattice when the produced strain is sufficiently small. If the ratio  $r(Ln)/r(Y)$ , at least for lanthanides with cation radius larger than that of Y, deviates from unit by less than 10%, it looks energetically more favoured for Ln to replace Y in Y-disilicates instead of a general rearrangement to form the new phase. Clear

Table 5  
Structural parameters ( $a, b, c, \beta, V, Z$ ), density ( $\rho_{XRD}$ ), and reliability index ( $R_{WP}$ ) for the Rietveld refinement of the high temperature new formed phases

| Compound                     | Lattice parameter |               |               |                 | Cell volume<br>( $\text{Å}^3$ ) | $Z^a$ | $\rho_{XRD}$<br>( $\text{g/cm}^3$ ) | $R_{WP}$<br>(%) | Ref.            |
|------------------------------|-------------------|---------------|---------------|-----------------|---------------------------------|-------|-------------------------------------|-----------------|-----------------|
|                              | $a(\text{Å})$     | $b(\text{Å})$ | $c(\text{Å})$ | $\beta(^\circ)$ |                                 |       |                                     |                 |                 |
| $(Y_{2/3}La_{1/3})_2Si_2O_7$ | 5.375(1)          | 8.569(1)      | 13.863(1)     | 111.79(1)       | 592.9                           | 4     | 4.250                               | 6.6             | [1]             |
| $(Y_{2/3}Ce_{1/3})_2Si_2O_7$ | 5.365(1)          | 8.509(1)      | 13.804(1)     | 111.45(1)       | 586.5                           | 4     | 4.305                               | 8.6             | TW <sup>b</sup> |
| $(Y_{1/2}Pr_{1/2})_2Si_2O_7$ | 5.370(1)          | 8.542(2)      | 13.838(2)     | 111.76(2)       | 589.6                           | 4     | 4.485                               | 8.6             | TW              |
| $(Y_{3/5}Nd_{2/5})_2Si_2O_7$ | 5.362(1)          | 8.496(1)      | 13.782(1)     | 111.46(1)       | 584.3                           | 4     | 4.435                               | 7.3             | TW              |

<sup>a</sup>  $Z$ : formula units per cell.

<sup>b</sup> TW: this work.

Table 6

X-ray diffraction data of the new phase  $(Y_{2/3}Ce_{1/3})_2Si_2O_7$  ( $I_{OBS} \geq 5$ )

| h | k | l  | d (Å)  | I calc | I obs | h | k | l  | d (Å)  | I calc | I obs |
|---|---|----|--------|--------|-------|---|---|----|--------|--------|-------|
| 0 | 1 | 1  | 7.094  | 454    | 396   | 1 | 3 | −5 | 1.9655 | 16     | 19    |
| 0 | 0 | 2  | 6.424  | 265    | 224   | 1 | 4 | 0  | 1.9571 | 28     | 31    |
| 0 | 1 | 2  | 5.127  | 54     | 43    | 1 | 1 | 5  | 1.9523 | 22     | 34    |
| 1 | 0 | 0  | 4.993  | 56     | 52    | 1 | 4 | −2 | 1.9517 | 6      | 9     |
| 1 | 0 | −2 | 4.907  | 17     | 11    | 2 | 3 | −2 | 1.9486 | 7      |       |
| 0 | 2 | 0  | 4.255  | 129    | 128   | 2 | 3 | −1 | 1.9317 | 18     | 19    |
| 1 | 1 | −2 | 4.251  | 16     | 130   | 1 | 1 | −7 | 1.9211 | 20     | 21    |
| 0 | 2 | 1  | 4.039  | 106    |       | 0 | 2 | 6  | 1.9127 | 10     | 12    |
| 0 | 1 | 3  | 3.825  | 36     | 28    | 0 | 4 | 3  | 1.9052 | 5      | 6     |
| 1 | 1 | 1  | 3.743  | 24     | 49    | 0 | 3 | 5  | 1.9043 | 15     | 18    |
| 1 | 1 | −3 | 3.670  | 14     | 32    | 1 | 4 | 1  | 1.8947 | 151    | 149   |
| 0 | 2 | 2  | 3.547  | 9      | 29    | 1 | 4 | −3 | 1.8851 | 155    | 149   |
| 1 | 0 | 2  | 3.388  | 738    | 774   | 2 | 3 | 0  | 1.8741 | 29     | 30    |
| 1 | 2 | −1 | 3.333  | 1000   | 1000  | 2 | 2 | 2  | 1.8715 | 153    | 157   |
| 1 | 0 | −4 | 3.307  | 941    | 943   | 2 | 3 | −4 | 1.8555 | 94     | 92    |
| 1 | 2 | 0  | 3.238  | 783    | 800   | 2 | 2 | −6 | 1.8351 | 164    | 196   |
| 1 | 2 | −2 | 3.214  | 523    | 625   | 2 | 1 | 3  | 1.8345 | 27     |       |
| 0 | 0 | 4  | 3.212  | 82     | 251   | 1 | 2 | 5  | 1.8143 | 180    | 194   |
| 1 | 1 | 2  | 3.147  | 240    |       | 1 | 3 | 4  | 1.8050 | 40     | 44    |
| 1 | 1 | −4 | 3.082  | 238    | 251   | 1 | 4 | 2  | 1.8015 | 39     | 43    |
| 0 | 2 | 3  | 3.018  | 439    | 488   | 0 | 1 | 7  | 1.7942 | 45     | 47    |
| 0 | 1 | 4  | 3.005  | 77     | 80    | 2 | 1 | −7 | 1.7918 | 6      | 6     |
| 1 | 2 | 1  | 2.977  | 5      | 5     | 1 | 2 | −7 | 1.7891 | 152    | 189   |
| 1 | 2 | −3 | 2.940  | 16     | 19    | 1 | 4 | −4 | 1.7891 | 31     |       |
| 0 | 3 | 1  | 2.770  | 114    | 114   | 2 | 3 | 1  | 1.7858 | 35     | 99    |
| 2 | 0 | −2 | 2.682  | 494    | 482   | 1 | 3 | −6 | 1.7843 | 62     |       |
| 1 | 2 | 2  | 2.650  | 55     | 306   | 3 | 0 | −2 | 1.7767 | 26     | 27    |
| 1 | 1 | 3  | 2.648  | 254    | 43    | 0 | 4 | 4  | 1.7736 | 58     | 57    |
| 1 | 2 | −4 | 2.611  | 46     |       | 2 | 3 | −5 | 1.7618 | 31     | 25    |
| 1 | 1 | −5 | 2.596  | 108    | 181   | 1 | 0 | 6  | 1.7498 | 21     | 20    |
| 0 | 3 | 2  | 2.595  | 103    | 136   | 3 | 1 | −2 | 1.7392 | 8      | 6     |
| 0 | 2 | 4  | 2.563  | 146    |       | 3 | 1 | −4 | 1.7280 | 6      | 6     |
| 2 | 1 | −2 | 2.558  | 13     | 13    | 1 | 0 | −8 | 1.7236 | 13     | 13    |
| 2 | 1 | −1 | 2.520  | 10     | 8     | 1 | 1 | 6  | 1.7140 | 76     | 89    |
| 1 | 3 | −1 | 2.507  | 8      | 8     | 2 | 0 | 4  | 1.6938 | 23     | 25    |
| 2 | 1 | −3 | 2.497  | 16     | 48    | 1 | 4 | 3  | 1.6908 | 63     | 66    |
| 2 | 0 | 0  | 2.497  | 31     | 179   | 1 | 1 | −8 | 1.6893 | 72     | 75    |
| 1 | 3 | 0  | 2.466  | 176    |       | 0 | 5 | 1  | 1.6871 | 21     | 23    |
| 0 | 1 | 5  | 2.460  | 97     | 96    | 3 | 1 | −5 | 1.6779 | 6      | 108   |
| 1 | 3 | −2 | 2.456  | 121    | 115   | 1 | 4 | −5 | 1.6771 | 113    |       |
| 2 | 1 | 0  | 2.396  | 31     | 22    | 3 | 0 | 0  | 1.6645 | 101    | 95    |
| 0 | 3 | 3  | 2.365  | 25     | 16    | 2 | 1 | 4  | 1.6612 | 23     | 21    |
| 2 | 1 | −4 | 2.357  | 16     | 10    | 2 | 4 | −1 | 1.6560 | 77     | 71    |
| 1 | 3 | 1  | 2.345  | 25     | 21    | 2 | 0 | −8 | 1.6535 | 30     | 28    |
| 1 | 0 | 4  | 2.340  | 6      | 6     | 2 | 4 | −3 | 1.6495 | 48     | 46    |
| 1 | 2 | 3  | 2.331  | 7      | 5     | 3 | 2 | −3 | 1.6482 | 164    | 155   |
| 1 | 0 | −6 | 2.295  | 72     | 75    | 3 | 2 | −2 | 1.6395 | 86     | 204   |
| 2 | 2 | −2 | 2.269  | 57     | 61    | 0 | 4 | 5  | 1.6386 | 105    |       |
| 2 | 2 | −1 | 2.242  | 38     | 43    | 1 | 3 | 5  | 1.6377 | 10     | 121   |
| 2 | 1 | −5 | 2.173  | 13     | 6     | 3 | 0 | −6 | 1.6355 | 117    |       |
| 2 | 2 | 0  | 2.153  | 171    | 176   | 3 | 2 | −4 | 1.6301 | 50     | 49    |
| 1 | 3 | −4 | 2.153  | 13     | 210   | 2 | 1 | −8 | 1.6232 | 44     | 44    |
| 0 | 0 | 6  | 2.141  | 175    |       | 1 | 3 | −7 | 1.6191 | 21     | 66    |
| 0 | 3 | 4  | 2.126  | 7      | 59    | 1 | 2 | 6  | 1.6183 | 43     |       |
| 2 | 2 | −4 | 2.125  | 52     | 354   | 1 | 5 | −2 | 1.6078 | 23     | 22    |
| 0 | 4 | 1  | 2.099  | 337    |       | 3 | 1 | −6 | 1.6061 | 30     | 29    |
| 2 | 0 | 2  | 2.084  | 6      | 6     | 1 | 2 | −8 | 1.5975 | 14     | 12    |
| 0 | 1 | 6  | 2.077  | 182    | 200   | 1 | 5 | 1  | 1.5755 | 64     | 54    |
| 1 | 2 | 4  | 2.050  | 44     | 45    | 1 | 4 | 4  | 1.5740 | 13     | 19    |
| 2 | 0 | −6 | 2.034  | 6      | 7     | 2 | 2 | 4  | 1.5737 | 9      |       |
| 2 | 1 | 2  | 2.024  | 74     | 526   | 1 | 5 | −3 | 1.5700 | 51     | 43    |
| 2 | 2 | 1  | 2.022  | 404    | 85    | 2 | 4 | 1  | 1.5612 | 11     | 12    |
| 1 | 2 | −6 | 2.020  | 37     |       | 1 | 4 | −6 | 1.5603 | 8      |       |
| 0 | 4 | 2  | 2.019  | 40     | 353   | 3 | 1 | 1  | 1.5523 | 28     | 20    |
| 2 | 2 | −5 | 1.9876 | 309    |       | 2 | 4 | −5 | 1.5451 | 6      | 5     |
| 1 | 3 | 3  | 1.9876 | 43     | 122   | 2 | 2 | −8 | 1.5412 | 8      | 38    |
| 2 | 1 | −6 | 1.9783 | 97     |       | 0 | 3 | 7  | 1.5409 | 31     |       |
| 1 | 4 | −1 | 1.9774 | 22     |       |   |   |    |        |        |       |

Table 7

Diffraction data of the new phase  $(Y_{1/2}Pr_{1/2})_2Si_2O_7$  ( $I_{OBS} \geq 5$ )

| h | k | l  | $d$ (Å) | $I$ calc | $I$ obs | h | k | l  | $d$ (Å) | $I$ calc | $I$ obs |
|---|---|----|---------|----------|---------|---|---|----|---------|----------|---------|
| 0 | 1 | 1  | 7.114   | 455      | 391     | 1 | 4 | -2 | 1.9590  | 8        | 9       |
| 0 | 0 | 2  | 6.426   | 244      | 217     | 1 | 1 | 5  | 1.9496  | 33       | 39      |
| 0 | 1 | 2  | 5.135   | 62       | 63      | 2 | 3 | -1 | 1.9350  | 6        | 7       |
| 1 | 0 | 0  | 4.987   | 37       | 48      | 1 | 1 | -7 | 1.9259  | 24       | 26      |
| 1 | 0 | -2 | 4.922   | 19       | 14      | 0 | 2 | 6  | 1.9147  | 5        | 7       |
| 1 | 1 | 0  | 4.307   | 20       | 11      | 0 | 4 | 3  | 1.9112  | 9        | 11      |
| 0 | 2 | 0  | 4.271   | 88       | 94      | 0 | 3 | 5  | 1.9080  | 12       | 15      |
| 1 | 1 | -2 | 4.264   | 39       |         | 1 | 4 | 1  | 1.8997  | 96       | 110     |
| 0 | 2 | 1  | 4.053   | 43       | 53      | 1 | 4 | -3 | 1.8923  | 109      | 126     |
| 0 | 1 | 3  | 3.829   | 34       | 20      | 2 | 3 | 0  | 1.8759  | 33       | 43      |
| 1 | 1 | 1  | 3.739   | 40       | 67      | 2 | 2 | 2  | 1.8695  | 105      | 118     |
| 1 | 1 | -3 | 3.684   | 27       | 41      | 2 | 3 | -4 | 1.8618  | 90       | 99      |
| 0 | 2 | 2  | 3.557   | 18       | 39      | 2 | 2 | -6 | 1.8418  | 72       | 115     |
| 1 | 0 | 2  | 3.380   | 811      | 843     | 2 | 1 | 3  | 1.8306  | 47       | 70      |
| 1 | 2 | -1 | 3.342   | 1000     | 1000    | 1 | 2 | 5  | 1.8131  | 136      | 191     |
| 1 | 0 | -4 | 3.319   | 899      | 892     | 1 | 3 | 4  | 1.8057  | 52       | 99      |
| 1 | 2 | 0  | 3.244   | 659      | 683     | 1 | 4 | 2  | 1.8053  | 24       |         |
| 1 | 2 | -2 | 3.226   | 484      | 496     | 2 | 1 | -7 | 1.7983  | 13       | 15      |
| 0 | 0 | 4  | 3.213   | 100      | 109     | 1 | 4 | -4 | 1.7958  | 34       | 184     |
| 1 | 1 | 2  | 3.143   | 198      | 212     | 0 | 1 | 7  | 1.7950  | 22       |         |
| 1 | 1 | -4 | 3.093   | 180      | 188     | 1 | 2 | -7 | 1.7940  | 114      |         |
| 0 | 2 | 3  | 3.025   | 514      | 525     | 1 | 3 | -6 | 1.7900  | 57       | 65      |
| 0 | 1 | 4  | 3.007   | 70       | 69      | 2 | 3 | 1  | 1.7864  | 40       | 48      |
| 0 | 3 | 1  | 2.780   | 72       | 100     | 0 | 4 | 4  | 1.7785  | 36       | 48      |
| 2 | 0 | -2 | 2.685   | 505      | 488     | 3 | 0 | -2 | 1.7771  | 6        | 8       |
| 1 | 2 | 2  | 2.650   | 68       | 67      | 2 | 3 | -5 | 1.7682  | 33       | 33      |
| 1 | 1 | 3  | 2.644   | 233      | 243     | 1 | 0 | 6  | 1.7473  | 27       | 18      |
| 1 | 2 | -4 | 2.621   | 31       | 30      | 3 | 1 | -4 | 1.7314  | 10       | 8       |
| 1 | 1 | -5 | 2.604   | 90       | 178     | 1 | 0 | -8 | 1.7274  | 10       | 7       |
| 0 | 3 | 2  | 2.603   | 103      |         | 1 | 1 | 6  | 1.7118  | 60       | 72      |
| 0 | 2 | 4  | 2.568   | 109      | 110     | 3 | 1 | -1 | 1.6979  | 6        | 6       |
| 2 | 1 | -2 | 2.561   | 31       | 30      | 0 | 5 | 1  | 1.6935  | 34       | 166     |
| 1 | 3 | -1 | 2.515   | 6        | 7       | 1 | 4 | 3  | 1.6935  | 78       |         |
| 2 | 1 | -3 | 2.503   | 27       | 30      | 1 | 1 | -8 | 1.6931  | 51       |         |
| 2 | 0 | 0  | 2.494   | 33       | 35      | 2 | 0 | 4  | 1.6898  | 23       | 22      |
| 1 | 3 | 0  | 2.473   | 133      | 134     | 1 | 4 | -5 | 1.6831  | 114      | 105     |
| 1 | 3 | -2 | 2.465   | 131      | 125     | 2 | 3 | 2  | 1.6792  | 11       | 10      |
| 0 | 1 | 5  | 2.461   | 131      | 133     | 3 | 0 | 0  | 1.6625  | 69       | 73      |
| 2 | 0 | -4 | 2.461   | 9        |         | 2 | 4 | -1 | 1.6597  | 64       | 115     |
| 2 | 1 | 0  | 2.394   | 23       | 23      | 2 | 0 | -8 | 1.6593  | 51       |         |
| 0 | 3 | 3  | 2.371   | 27       | 25      | 2 | 1 | 4  | 1.6577  | 30       | 29      |
| 2 | 1 | -4 | 2.365   | 11       | 10      | 2 | 4 | -3 | 1.6548  | 45       | 43      |
| 1 | 3 | 1  | 2.349   | 19       | 16      | 3 | 2 | -3 | 1.6506  | 154      | 150     |
| 1 | 2 | -5 | 2.303   | 9        | 49      | 0 | 4 | 5  | 1.6426  | 62       | 66      |
| 1 | 0 | -6 | 2.302   | 43       |         | 3 | 2 | -2 | 1.6408  | 76       | 191     |
| 2 | 2 | -2 | 2.273   | 27       | 41      | 3 | 0 | -6 | 1.6405  | 100      |         |
| 2 | 2 | -1 | 2.244   | 16       | 24      | 1 | 3 | 5  | 1.6379  | 4        | 5       |
| 2 | 1 | -5 | 2.181   | 15       | 5       | 3 | 2 | -4 | 1.6336  | 42       | 46      |
| 1 | 3 | -4 | 2.161   | 9        | 6       | 3 | 1 | 0  | 1.6318  | 6        | 7       |
| 2 | 2 | 0  | 2.153   | 141      | 135     | 2 | 1 | -8 | 1.6288  | 27       | 29      |
| 0 | 0 | 6  | 2.142   | 154      | 173     | 1 | 3 | -7 | 1.6238  | 24       | 26      |
| 2 | 2 | -4 | 2.132   | 52       | 51      | 2 | 4 | 0  | 1.6220  | 6        | 6       |
| 0 | 3 | 4  | 2.131   | 17       | 17      | 1 | 2 | 6  | 1.6172  | 40       | 45      |
| 0 | 4 | 1  | 2.107   | 285      | 283     | 1 | 5 | -2 | 1.6139  | 8        | 9       |
| 2 | 0 | 2  | 2.079   | 5        | 189     | 2 | 4 | -4 | 1.6129  | 5        | 5       |
| 0 | 1 | 6  | 2.078   | 168      |         | 3 | 1 | -6 | 1.6111  | 16       | 16      |
| 1 | 2 | 4  | 2.049   | 28       | 25      | 1 | 2 | -8 | 1.6014  | 13       | 13      |
| 0 | 4 | 2  | 2.027   | 47       | 95      | 1 | 5 | 1  | 1.5802  | 61       | 47      |
| 1 | 2 | -6 | 2.026   | 49       |         | 1 | 5 | -3 | 1.5760  | 54       | 59      |
| 2 | 2 | 1  | 2.021   | 365      | 443     | 1 | 4 | 4  | 1.5760  | 6        |         |
| 2 | 1 | 2  | 2.020   | 40       |         | 2 | 2 | 4  | 1.5713  | 7        | 6       |
| 2 | 2 | -5 | 1.9948  | 257      | 269     | 2 | 4 | -5 | 1.5509  | 7        | 31      |
| 1 | 3 | 3  | 1.9891  | 25       | 24      | 3 | 1 | 1  | 1.5499  | 21       |         |
| 2 | 1 | -6 | 1.9855  | 77       | 106     | 3 | 2 | 0  | 1.5492  | 6        |         |
| 1 | 4 | -1 | 1.9843  | 26       |         | 2 | 2 | -8 | 1.5467  | 7        | 7       |
| 1 | 3 | -5 | 1.9723  | 9        | 12      | 2 | 3 | -7 | 1.5451  | 5        | 5       |
| 1 | 4 | 0  | 1.9631  | 23       | 25      | 0 | 3 | 7  | 1.5430  | 33       | 36      |



Table 8  
Diffraction data of the new phase ( $\text{Y}_{3/5}\text{Nd}_{2/5}\text{Si}_2\text{O}_7$  ( $I_{\text{OBS}} \geq 5$ ))

| h | k | l  | $d$ (Å) | $I$ calc | $I$ obs | h | k | l  | $d$ (Å) | $I$ calc | $I$ obs |
|---|---|----|---------|----------|---------|---|---|----|---------|----------|---------|
| 0 | 1 | 1  | 7.083   | 396      | 352     | 2 | 1 | −6 | 1.9760  | 59       | 102     |
| 0 | 0 | 2  | 6.413   | 218      | 199     | 1 | 4 | −1 | 1.9746  | 35       |         |
| 0 | 1 | 2  | 5.119   | 76       | 86      | 1 | 3 | −5 | 1.9625  | 9        | 12      |
| 1 | 0 | 0  | 4.990   | 29       | 41      | 1 | 4 | 0  | 1.9543  | 14       | 20      |
| 1 | 0 | −2 | 4.903   | 27       | 21      | 1 | 1 | 5  | 1.9495  | 12       | 37      |
| 1 | 1 | −1 | 4.533   | 4        | 7       | 1 | 4 | −2 | 1.9489  | 11       |         |
| 1 | 1 | 0  | 4.303   | 34       | 36      | 2 | 3 | −2 | 1.9466  | 4        | 6       |
| 0 | 2 | 0  | 4.248   | 145      | 140     | 2 | 3 | −1 | 1.9298  | 28       | 32      |
| 1 | 1 | −2 | 4.246   | 22       |         | 2 | 3 | −3 | 1.9194  | 4        | 5       |
| 0 | 2 | 1  | 4.033   | 114      | 130     | 1 | 1 | −7 | 1.9180  | 4        | 5       |
| 1 | 1 | 1  | 3.739   | 51       | 57      | 0 | 2 | 6  | 1.9096  | 11       | 12      |
| 1 | 1 | −3 | 3.666   | 40       | 58      | 0 | 3 | 5  | 1.9013  | 7        | 7       |
| 0 | 2 | 2  | 3.542   | 13       | 29      | 1 | 4 | 1  | 1.8921  | 149      | 138     |
| 1 | 0 | 2  | 3.384   | 794      | 802     | 1 | 4 | −3 | 1.8823  | 161      | 149     |
| 1 | 2 | −1 | 3.329   | 947      | 956     | 2 | 3 | 0  | 1.8722  | 49       | 51      |
| 1 | 0 | −4 | 3.303   | 1000     | 1000    | 2 | 2 | 2  | 1.8696  | 129      | 134     |
| 1 | 2 | 0  | 3.235   | 614      | 632     | 2 | 3 | −4 | 1.8534  | 86       | 85      |
| 1 | 2 | −2 | 3.210   | 487      | 555     | 2 | 2 | −6 | 1.8328  | 149      | 205     |
| 0 | 0 | 4  | 3.207   | 35       |         | 2 | 1 | 3  | 1.8326  | 36       |         |
| 1 | 1 | 2  | 3.144   | 234      | 252     | 1 | 2 | 5  | 1.8117  | 174      | 207     |
| 1 | 1 | −4 | 3.078   | 155      | 156     | 1 | 3 | 4  | 1.8024  | 42       | 43      |
| 0 | 2 | 3  | 3.013   | 482      | 511     | 1 | 4 | 2  | 1.7990  | 28       | 30      |
| 0 | 1 | 4  | 3.000   | 49       | 47      | 0 | 1 | 7  | 1.7912  | 46       | 49      |
| 0 | 3 | 1  | 2.765   | 64       | 76      | 2 | 1 | −7 | 1.7895  | 5        | 5       |
| 2 | 0 | −2 | 2.680   | 514      | 547     | 1 | 4 | −4 | 1.7864  | 19       | 192     |
| 1 | 2 | 2  | 2.647   | 59       | 273     | 1 | 2 | −7 | 1.7863  | 171      |         |
| 1 | 1 | 3  | 2.644   | 191      |         | 2 | 3 | 1  | 1.7839  | 41       | 41      |
| 1 | 2 | −4 | 2.607   | 26       | 29      | 1 | 3 | −6 | 1.7815  | 36       | 36      |
| 1 | 1 | −5 | 2.592   | 68       | 195     | 3 | 0 | −2 | 1.7758  | 9        | 9       |
| 0 | 3 | 2  | 2.591   | 141      |         | 0 | 4 | 4  | 1.7708  | 49       | 44      |
| 0 | 2 | 4  | 2.559   | 141      | 141     | 2 | 3 | −5 | 1.7597  | 13       | 6       |
| 2 | 1 | −2 | 2.556   | 33       | 32      | 1 | 0 | 6  | 1.7474  | 13       | 5       |
| 2 | 1 | −1 | 2.518   | 6        | 9       | 3 | 1 | −2 | 1.7382  | 14       | 8       |
| 2 | 1 | −3 | 2.495   | 39       | 86      | 1 | 0 | −8 | 1.7208  | 12       | 6       |
| 2 | 0 | 0  | 2.495   | 42       |         | 1 | 1 | 6  | 1.7114  | 48       | 55      |
| 1 | 3 | 0  | 2.463   | 193      | 194     | 2 | 0 | 4  | 1.6919  | 24       | 25      |
| 0 | 1 | 5  | 2.456   | 81       | 79      | 1 | 4 | 3  | 1.6883  | 67       | 69      |
| 1 | 3 | −2 | 2.452   | 138      | 133     | 1 | 1 | −8 | 1.6865  | 54       | 56      |
| 2 | 0 | −4 | 2.451   | 5        | 5       | 0 | 5 | 1  | 1.6845  | 23       | 24      |
| 2 | 1 | 0  | 2.394   | 17       | 21      | 3 | 1 | −5 | 1.6766  | 5        | 5       |
| 0 | 3 | 3  | 2.361   | 20       | 21      | 1 | 4 | −5 | 1.6746  | 109      | 96      |
| 2 | 1 | −4 | 2.355   | 31       | 27      | 3 | 0 | 0  | 1.6634  | 84       | 84      |
| 1 | 3 | 1  | 2.342   | 13       | 15      | 2 | 1 | 4  | 1.6594  | 30       | 30      |
| 1 | 0 | −6 | 2.292   | 71       | 75      | 2 | 4 | −1 | 1.6541  | 67       | 64      |
| 2 | 2 | −2 | 2.267   | 16       | 17      | 2 | 0 | −8 | 1.6513  | 55       | 51      |
| 1 | 1 | 4  | 2.253   | 5        | 6       | 2 | 4 | −3 | 1.6475  | 36       | 164     |
| 2 | 2 | −1 | 2.240   | 21       | 23      | 3 | 2 | −3 | 1.6470  | 141      |         |
| 2 | 1 | 1  | 2.217   | 6        | 6       | 3 | 2 | −2 | 1.6384  | 86       | 88      |
| 1 | 1 | −6 | 2.213   | 15       | 15      | 0 | 4 | 5  | 1.6360  | 95       | 115     |
| 2 | 2 | 0  | 2.151   | 137      | 143     | 1 | 3 | 5  | 1.6353  | 14       |         |
| 1 | 3 | −4 | 2.150   | 6        |         | 3 | 0 | −6 | 1.6342  | 136      | 144     |
| 0 | 0 | 6  | 2.138   | 191      | 220     | 3 | 1 | 0  | 1.6324  | 12       | 12      |
| 2 | 2 | −4 | 2.123   | 42       | 68      | 3 | 2 | −4 | 1.6289  | 43       | 43      |
| 0 | 3 | 4  | 2.123   | 23       |         | 2 | 1 | −8 | 1.6210  | 26       | 25      |
| 0 | 4 | 1  | 2.095   | 280      | 318     | 2 | 4 | 0  | 1.6174  | 6        | 85      |
| 2 | 0 | 2  | 2.082   | 5        | 6       | 1 | 3 | −7 | 1.6166  | 20       |         |
| 0 | 1 | 6  | 2.073   | 153      | 170     | 1 | 2 | 6  | 1.6159  | 59       |         |
| 1 | 2 | 4  | 2.047   | 35       | 21      | 1 | 5 | −2 | 1.6055  | 10       | 22      |
| 2 | 0 | −6 | 2.032   | 13       | 14      | 2 | 4 | −4 | 1.6052  | 2        |         |
| 2 | 1 | 2  | 2.022   | 57       | 472     | 3 | 1 | −6 | 1.6048  | 9        |         |
| 2 | 2 | 1  | 2.020   | 365      |         | 1 | 2 | −8 | 1.5949  | 24       | 17      |
| 1 | 2 | −6 | 2.017   | 37       | 66      | 1 | 5 | 1  | 1.5733  | 47       | 32      |
| 0 | 4 | 2  | 2.016   | 25       |         | 1 | 5 | −3 | 1.5676  | 45       | 30      |
| 2 | 2 | −5 | 1.9854  | 268      | 328     | 3 | 1 | 1  | 1.5511  | 35       | 10      |
| 1 | 3 | 3  | 1.9848  | 44       |         | 2 | 4 | −5 | 1.5432  | 8        | 5       |

evidence of this phenomenon was supplied by SEM investigations and XRD determination of the modified lattice parameters.

## References

1. Monteverde, F. and Celotti, G., Structural data from X-ray powder diffraction of a new phase formed in the  $\text{Si}_3\text{N}_4\text{-La}_2\text{O}_3\text{-Y}_2\text{O}_3$  system after oxidation in air. *J. Eur. Ceram. Soc.*, 1999, **19**, 2021–2026.
2. Greis, O., Bossemeyer, H. G., Greil, P., Breidenstein, B. and Haase, A., Structural data of the monoclinic high-temperature G-form of  $\text{La}_2\text{Si}_2\text{O}_7$  from X-ray powder diffraction. *Materials Science Forum*, 1991, **79-82**, 803–808.
3. Cuneit Tas, A. and Akinc, M., Crystal structures of the high-temperature forms of  $\text{Ln}_2\text{Si}_2\text{O}_7$  (Ln = La, Ce, Pr, Nd, Sm) revisited. *J. Am. Cer. Soc.*, 1994, **77**(11), 2968–2970.
4. Young, R. A., Sakthivel, A., Moss, T. S. and Paiva-Santos, C. O., *DBWS-9411, Rietveld analysis of X-ray and neutron powder diffraction patterns*. Georgia Institute of Technology, Atlanta, 1995.
5. Marciniak, H., *DMPLLOT, Plot View Program for Rietveld Refinement Method*. High Pressure Research Centre, Warsaw, 1995.
6. Kraus, W. and Nolze, G., *PowderCell for Windows 2.3*. Federal Institute for Materials Research and Testing, Berlin, 1999.
7. Liddell, K. and Thompson, D. P., X-ray diffraction data for Yttrium silicates. *Br. Ceram. Trans. J.*, 1986, **85**, 17–22.